

Developing a Coupled Static-Dynamic Algorithm for Optimization of Reservoir Characterization

S. K. Abolfazli, B. Tokhmechi, S. R. Ghavami Riabi

Faculty of Mining, Petroleum and Geophysics Engineering, Shahrood University of Technology, Shahrood, Iran

Received February 28, 2022, Accepted October 14, 2022

Abstract

Reservoir simulation is the combination of physics, mathematics, reservoir engineering, and computer programming for predicting the performance of a hydrocarbon reservoir under various operating conditions. The necessity of optimizing oil extraction methods is to increase the efficiency of a hydrocarbon reservoir under various operating conditions. Therefore, in a hydrocarbon recovery project that may involve hundreds of millions of dollars in investments, the risk associated with using the best method for the desired outcome must be evaluated and minimized.

Finding an optimal model for static reservoir simulation through fluid flow model is the main goal of this paper. For this purpose, first of all, artificial data of porosity and permeability was generated, and then these data were used for geostatistical simulation. Sequential Gaussian Simulation (SGS) method was used for static simulation of a region and for each of two static parameters, 25 realizations were obtained. The realizations of SGS were randomly entered in the dynamic model of the reservoir. Dynamic model was coded by Python for slightly-compressible fluid flow equations in three dimensions and the pressure in each of the blocks in the oil production reservoir was determined. For each category, the least Sum of Squared Errors (SSE) was determined and then the corresponding static model was selected as the desired static model. With a reliable static model, it is possible to define different locations for designing injection and oil production wells, potential intelligent wells areas, as well as optimizing the management of a reservoir, which leads to costs reduction and, at the same time, increase in oil production.

Keywords: *Static modeling; Sequential Gaussian simulation; Dynamic modeling; Slightly-compressible fluid flow equations; Integrated reservoir Modeling; History matching.*

1. Introduction

Reservoir simulation is a numerical model in the petroleum industry that has become a pattern for solving reservoir engineering problems. In fact, reservoir simulation is the operation of simulating the department of fluid flow in porous media of an oil reservoir and predicting the performance of a hydrocarbon reservoir using the combining physics, mathematics and reservoir engineering. A reservoir simulation model is a suitable tool for reducing the costs of multi-million dollar investments by predicting the performance of oil reservoir and location of wells. This model is created from initial parameters, then certify through the history matching method. History matching is done to bring the performance of simulation model closer to the performance of actual reservoir [1].

In predicting the reservoir study, it is important to help the decision-making process by a positive impact on the technical and business performance of oil industry. History matching is one of the most important of methods, which helps greatly in the optimization of the field. History matching is also calibrated based on historical observations and used to estimate future hydrocarbon production [2].

Due to the large resources and errors in the input data, building a model without a history match will not be accurate enough in the results. Nowadays, with the advantage of computer

science, the methods of history matching are performed with better quality and less computation and time than traditional methods [3].

Reservoir simulation is an important part and should be done with the least error, which still needs more attention and discussion. One of the essential tasks for describing the reservoir is the integration of two important datasets called static and dynamic data. Static data such as porosity and permeability are obtained from the core, log, and seismic data. Dynamic data include pressure, saturation, and fluid rates. The integration method increases quality of the reservoir models and reduces the uncertainty of the simulated models [4].

Mathematical methods are the most appropriate methods for integrating static and dynamic data, and are divided into three categories: deterministic or gradient-based methods [5-6], stochastic methods and particle filter methods. In last two decades, there have been many activities to develop stochastic methods by using history matching. These methods do not use gradient information. In short, it uses the trial and error approach in the manual reservoir model structure system. The most commonly used methods are: on simulated annealing and genetic algorithms [7-8].

The convergence rate of deterministic methods is faster than stochastic methods, but one of the good advantages of stochastic methods is the easier computational performance and lower computational volume. Stochastic methods are classified as global optimization algorithms. Instead of minimizing the target locale, these methods attempt to achieve the global minimum of the objective function. However, it should be noted that the number of iterations is limited and access to the global minimum may be difficult.

Previously used of history matching are genetic algorithm [9-10], particle swarm optimization (PSO) [11-12], evolutionary strategies [13], ant colony optimization (ACO) [14], Gaussian Process [15], genetic algorithm and particle swarm optimization [16]. Deterministic methods calculate the gradients of the mathematical model with regards to the parameters (permeability, porosity, e.g.) and minimize the objective function [17-18].

As previously mentioned, these methods have a very quick convergence rate to a local minimum of the objective function. However, they also have weaknesses, for example in many conditions these algorithms may not converge to a local minimum [4]. Bayesian framework [19], and LBFGS algorithm [20-21] are some examples.

Finally, The Kalman filter is an estimator that uses the previous state estimation and the current observation to calculate the current state estimation as powerful tool for combining information in the presence of uncertainties. The measurements are also associated with uncertainty [22]. The EnKF is based on the simpler Kalman filter [23-24]. The extended Kalman filter has also been used for parameter estimation in hydrological modeling [25-26].

The main approach of this paper is to develop an optimization phase in a simulated model to find the optimal simulated static model for improving oil production with a combination of static and dynamic simulation techniques in uncertain geological scenarios.

2. Materials and methods

2.1. Static reservoir simulation

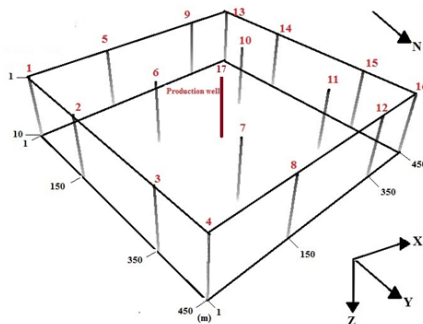


Figure 1. Position of wells in 3D view

Porosity and permeability are the most important petrophysical properties of the reservoir. A synthetic $450 \times 450 \times 6$ heterogeneous reservoir is generated comprising 600 cells ($10 \times 10 \times 6$). In Table 1, detail information about the number of blocks in three axes of X, Y, and Z, as well as the size of the blocks are provided. Petrophysical and fluid properties data is generated using normal and random conditions. The position and three-dimensional arrangement of wells are mentioned in Figure 1. Table 2 is given the maximum, minimum, mean and variance values of porosity and permeability.

Table 1. Properties of the grid embedded in the study area in three directions X, Y and Z

	Y-direction	X-direction	Z-direction
Number of blocks	10	10	10
Block size	45 m	45 m	1 m

Table 2. Statistical data information

Variable name	Porosity (%)	Permeability (md)
minimum	7.9864	32.5083
Maximum	23.9531	83.7347
Mean	15.99	57.97
Variance	3.9842	35.828

The SGS geostatistical method is used in the current article to construct the static model and generated 25 permeability, porosity, field realizations of a 3D reservoir. Some of these realizations are shown in Figure 2.

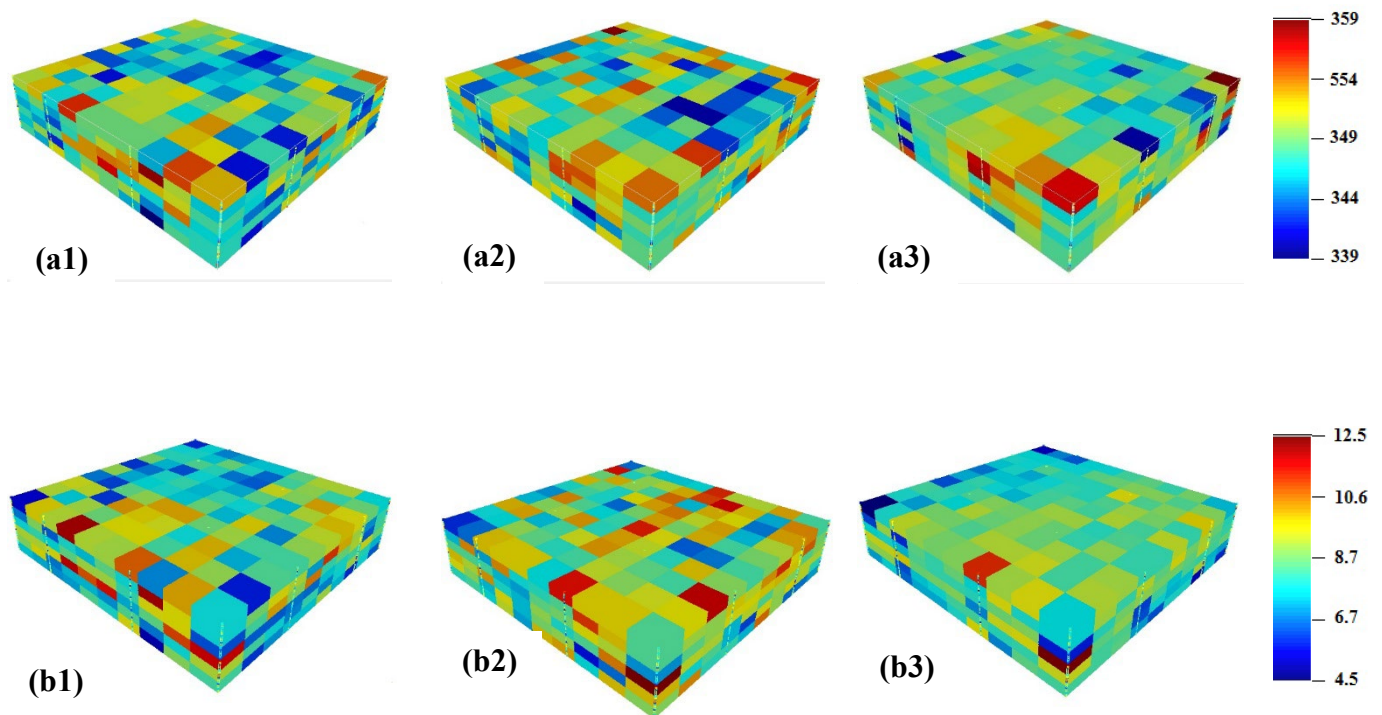


Figure 2. Realization of SGS method. a) Permeability, b) Porosity. Numbers one and two are two realizations of 25 realizations and numbers three are the average model of 25 realizations

2.2. Fluid flow simulation

Mathematical modeling of a system needs to understand the behavior of different components that build a system. In the reservoir simulation, system is composed of reservoir rocks and various fluids that flow through it. For model developers and users, a complete understanding of the relationship between fluid densities, viscosity, formation volume factor, soluble gas/liquid to pressure ratios, and also relative permeability and capillary pressure with saturation are very useful.

Several numerical methods are used to discretization fluid flow equations. The most common approach in the oil industry is the finite-difference approximation [27-28]. Slightly-compressible fluid flow equation is expressed in three dimensions according to Equation 1:

$$\begin{aligned} & \frac{\partial}{\partial x} \left(\frac{\beta_c A_x k_x}{\mu_l B_l} \frac{\partial \Phi_l}{\partial x} \right) \Delta x + \\ & \frac{\partial}{\partial y} \left(\frac{\beta_c A_y k_y}{\mu_l B_l} \frac{\partial \Phi_l}{\partial y} \right) \Delta y + \\ & \frac{\partial}{\partial z} \left(\frac{\beta_c A_z k_z}{\mu_l B_l} \frac{\partial \Phi_l}{\partial z} \right) \Delta z + \\ & q_{lsc} = \frac{V_b \phi c_l}{\alpha_c B_l} \frac{\partial p}{\partial t} \end{aligned} \tag{Eq. 1}$$

where $l = o$ or w ; β_c is a unit coefficient equal to 0.001127; k_x , k_y and k_z are the absolute permeability of the rock in the flow direction; A_x , A_y and A_z are introduced as area perpendicular to flow. Respectively q_{sc} , V , ϕ , B_l are called the production rate in standard term, the volume of each block, the porosity of each block, the formation volume factor; α_c , is as a constant value, in this case equal to 5.615; c_l is the total oil compressibility calculated using Equation 2:

$$C_o = S_w C_w + (1 - S_w) C_o + C_r \tag{Eq. 2}$$

In Equation 1, Φ is called the potential gradient and defined by Equation 3 and γ_l is the density of the liquid phase. P and Z are optional points of pressure and height, respectively.

$$\vec{\nabla} \Phi_l = \vec{\nabla} p - \gamma_l \vec{\nabla} Z \tag{Eq. 3}$$

The presence of a third dimension creates a coefficient matrix with a heptadiagonal structure for the three-dimensional problem. Figure 3 shows the matrix equation for three-axes flow. By replacing Equation 3 into Equation 1 and applying the backward difference approximation, the result will be as follow [27, 29-31]:

$$\begin{aligned} & B_{i,j,k} p_{i,j,k-1}^{n+1} + S_{i,j,k} p_{i,j-1,k}^{n+1} + W_{i,j,k} p_{i-1,j,k}^{n+1} + C_{i,j,k} p_{i,j,k}^{n+1} + E_{i,j,k} p_{i+1,j,k}^{n+1} + N_{i,j,k} p_{i,j+1,k}^{n+1} + \\ & A_{i,j,k} p_{i,j,k+1}^{n+1} = Q_{i,j,k} \end{aligned} \tag{Eq. 4}$$

In the simpler form of this equation is Equation 5:

$$\underline{M} \times \underline{P} = \underline{Q} \tag{Eq. 5}$$

$$A_{i,j,k} = T_{lz_{i,j,k+\frac{1}{2}}} \tag{Eq. 6}$$

$$N_{i,j,k} = T_{ly_{i,j+\frac{1}{2},k}} \tag{Eq. 7}$$

$$E_{i,j,k} = T_{lx_{i+\frac{1}{2},j,k}} \tag{Eq. 8}$$

$$B_{i,j,k} = T_{lz_{i,j,k-\frac{1}{2}}} \tag{Eq. 9}$$

$$S_{i,j,k} = T_{ly_{i,j-\frac{1}{2},k}} \tag{Eq. 10}$$

$$W_{i,j,k} = T_{lx_{i-\frac{1}{2},j,k}} \tag{Eq. 11}$$

where \underline{M} is the $n \times n$ matrix of transmissibility; \underline{P} display a vector of unknown-block pressures; and \underline{Q} is introduced as vector of boundary condition.

The equations used for calculating the components of Equation 4 are as follow: The coefficient C is the principal diameter of the matrix, which is calculated by Equation 12.

$$C_{i,j,k} = - \left[\begin{aligned} & B_{i,j,k} + S_{i,j,k} + W_{i,j,k} + E_{i,j,k} \\ & + N_{i,j,k} + A_{i,j,k} + \left(\frac{V_b \phi c_l}{\alpha_c B_l \Delta t} \right)_{i,j,k} \end{aligned} \right] \tag{Eq. 12}$$

Also, the value of T is used to define the coefficients A, N, E, B, S, W, known as the transpiration coefficient, and represented by Equation 13:

$$T_{lx,y,z_{i,j,k}} = \left(\beta_c \frac{A_x k_x}{\mu_l B_l \Delta x} \right)_{i,j,k} \tag{Eq. 13}$$

The value of $Q_{i,j,k}$ as gravity- head term ($\gamma_l Z$) is calculated by Equation 14.

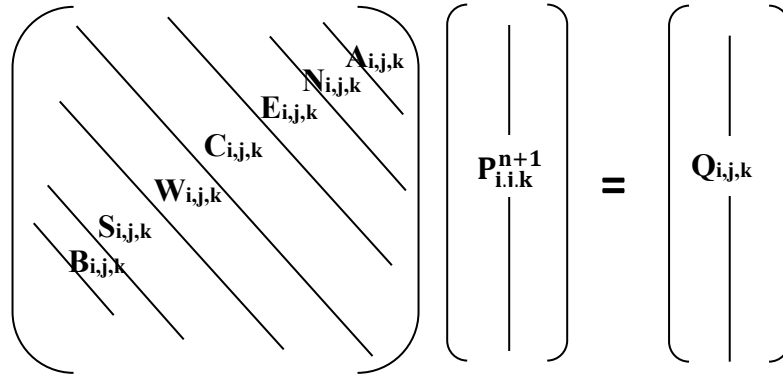


Figure 1. Schematic representation of the matrix generated by the 3D, slightly- compressible- flow equation

$$Q_{i,j,k} = - \left(\frac{V_b \phi c_l}{\alpha_c B_l \Delta t} \right)_{i,j,k} p_i^n - q_{lsc_{i,j,k}} + B_{i,j,k} \gamma_{l_{i,j,k-\frac{1}{2}}} (Z_{i,j,k-1} - Z_{i,j,k}) + S_{i,j,k} \gamma_{l_{i,j-\frac{1}{2},k}} (Z_{i,j-1,k} - Z_{i,j,k}) + W_{i,j,k} \gamma_{l_{i-\frac{1}{2},j,k}} (Z_{i-1,j,k} - Z_{i,j,k}) + E_{i,j,k} \gamma_{l_{i+\frac{1}{2},j,k}} (Z_{i+1,j,k} - Z_{i,j,k}) + N_{i,j,k} \gamma_{l_{i,j+\frac{1}{2},k}} (Z_{i,j+1,k} - Z_{i,j,k}) + A_{i,j,k} \gamma_{l_{i,j,k+\frac{1}{2}}} (Z_{i,j,k+1} - Z_{i,j,k}) \tag{Eq. 14}$$

P_i^n and $q_{lsc_{i,j,k}}$ are the pressure and injection/production in each block, respectively.

2.3. Solver: Gaussian elimination

In the previous sections, equation 5 was introduced, that is a multi-equation. The Gaussian elimination method is one of the most popular and well-known methods for solving equations simultaneously. This method consists of forward elimination and backward substitution.

Forward elimination: The purpose of the forward elimination is to create an upper triangular matrix, which is used as primary operators to achieve its goal.

The first step assign augmented matrix of M, denoted as \tilde{M} , by inserting Q in M as last column:

$$\tilde{M} = \begin{bmatrix} m_{11} & m_{12} & \cdots & m_{1n} & q_1 \\ m_{21} & m_{22} & \cdots & m_{2n} & q_2 \\ \vdots & \vdots & \vdots & \vdots & \vdots \\ m_{n1} & m_{n2} & & m_{nn} & q_n \end{bmatrix} = \begin{bmatrix} P_1 \\ P_2 \\ \vdots \\ P_n \end{bmatrix}$$

In this level, unknown parameters as like pressure in each cell are systematically deleted from the matrix equation. Assume that the first k^{th} rows of the matrix \tilde{M}' are upper triangular matrix form, therefore, the pivot equation is the k. And all the equations below it still need to be converted. The i^{th} row is below the pivot equation and the m_{ik} element must be deleted. In this method, the difference of an equation (i equation) and the result of multiplying another equation (j equation) and constant $\lambda = m_{ik}/m_{kk}$ is used to reach its goal.

$$\begin{bmatrix} m_{11} & m_{12} & \cdots & m_{1k} & \cdots & m_{1j} & \cdots & m_{1n} & b_1 \\ 0 & m_{22} & \cdots & m_{2k} & \cdots & m_{2j} & \cdots & m_{2n} & b_2 \\ \vdots & \vdots & & \vdots & & \vdots & & \vdots & \vdots \\ 0 & 0 & \cdots & m_{kk} & \cdots & m_{kj} & \cdots & m_{kn} & b_k \\ \vdots & \vdots & & \vdots & & \vdots & & \vdots & \vdots \\ 0 & 0 & \cdots & m_{ik} & \cdots & m_{ij} & \cdots & m_{in} & b_i \\ \vdots & \vdots & & \vdots & & \vdots & & \vdots & \vdots \\ 0 & 0 & \cdots & m_{nk} & \cdots & m_{nj} & \cdots & m_{nn} & b_n \end{bmatrix}$$

The corresponding changes in the i^{th} row are as follows:

$$\begin{aligned} m_{ij} &\leftarrow m_{ij} - \lambda m_{kj} & j &= k, k + 1, \dots, n \\ b_i &\leftarrow b_i - \lambda b_k & i &= k + 1, k + 2, \dots, n \\ & & k &= 1, 2, \dots, n - 1 \end{aligned}$$

Backward substitution: the last unknown parameters is obtained from the last equation and other unknown resolved by substituting known values into the upper triangular matrix equation. Repeat the back-substitute processes to obtain a unique answer.

3. Results

3.1. Integration of static and dynamic models

In the previous sections, static and fluid flow models are explained. This section describes how to integrate the two models to obtain the pressure in each reservoir block.

From each of the two class (porosity, permeability) realizations, SGS was randomly entered in dynamic model, the method of importing static models into code helps user to control numbers of models, depending cost, time and their system of computer.

In this research, 25 static models separately made for porosity and permeability. Only 20% of them in two steps imported into code. 5 models imported from porosity and 5 models from permeability. Making a dynamic model of reservoir needs a porosity model and a permeability model, after running the code and calculating pressure on each grid block, sum of square error (SSE) will be calculated

The Sum of Squared Errors (SSE) was calculated by Equation 16:

$$SSE = \sum (y_i - y'_i)^2 \tag{Eq. 16}$$

y_i is the output value for the actual model and y'_i is the answer obtained from the simulated model. In this paper, y'_i is the amount of pressure obtained for each grid block, and using artificial data, and the actual amount equal to the amount of pressure that is intended 4175 Pisa.

Importing static models of porosity and permeability was random. At first step one of porosity models imported into the code and fixed, by every code running one of five permeability models imported to the code. For each model, it's SEE and block's pressures calculated. Each step after calculating current SEE and it deducted with pervious SEEs by coding and models related to them choose as desirable model. After importing all permeability models, the model with lowest SEE choose as fixed desirable model.

On the next step porosity models were variable and sequentially imported to the code and like the first step, pressure of each block and SEEs of them were calculated.

New SEE and pervious SEEs deducted and models with lowest SEE's introduced as desirable models with due attention to choosing 5 porosity models and 5 permeability models and the way of importing static models , at last the code ran 9 times and 9 models obtained and for each one SEE and pressure calculated separately.

The performance of this part and the fluid flow model is obtained through coding in the Python software. Figure 4 is shown the flowchart that describes the different steps of the coding algorithm.

Figure 2. Flowchart of fluid flow simulation code in porous media

3.2. Comparison of SSE, production index and bottom hole pressure

In Figure 5, the SSE for the nine dynamic model is illustrated. In Figure 5a, the static model is a constant porosity and changes due to various permeability models so the reason for the change in the SSE and pressures is the change in the permeability models. The SSE of number 4 with quantity 27450.7 less than the others so permeability model of it, is desirable model for next step.

Figure 5b is the results of fixed desirable permeability and difference porosity models. By increasing pressure, quantity of SEEs decreased. Considering Figure 5b, SEEs increased and model number 4 with lowest SEE choose as desirable model. Most SSE belong to models 1 and 3.

In Figure 6, the pressure of the production well in their cells for nine different dynamic models was shown that the pressure chart for model 4 is higher than other models and has higher values. Bottom hole pressure and drawdown values are shown in Table 3. The highest bottom hole pressure with 3758.88 Psi and minimum drawdown 416.12 Psi, belongs to dynamic model number 4.

Table 3. BHP, PI and draw down values for 9 models

Number of model	BHP (psi)	Draw down	PI
1	3731.28	443.72	0.901
2	3748.34	426.66	0.938
3	3746.21	428.79	0.933
4	3758.89	416.11	0.961
5	3750.72	424.28	0.943
6	3756.69	418.31	0.956
7	3755.25	419.75	0.953
8	3756.21	418.79	0.955
9	3754.57	420.73	0.951

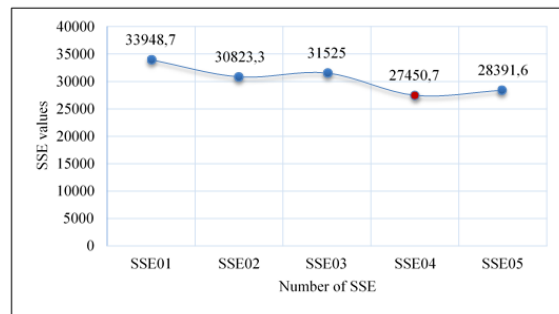


Figure 5. SSE values for 9 different models. 5a) changes due to permeability models. 5b) changes due to porosity models

On the other side Models 1 and 3 have the lowest values with 3731.28 and 3746.21 Psi, respectively. The drawdown for these models is at the highest value and is equal to 443.72 and 428.79. Figure 7 shows the static models of porosity and permeability corresponding to model 4.

Figure 5. SSE values for 9 different models. 5a) changes due to permeability models. 5b) changes due to porosity models

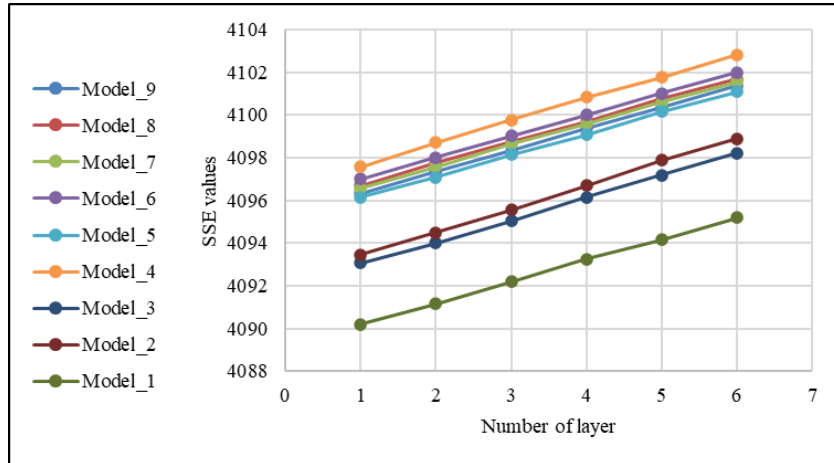


Figure 6. Pressure of the production well in their cells for 9 different models

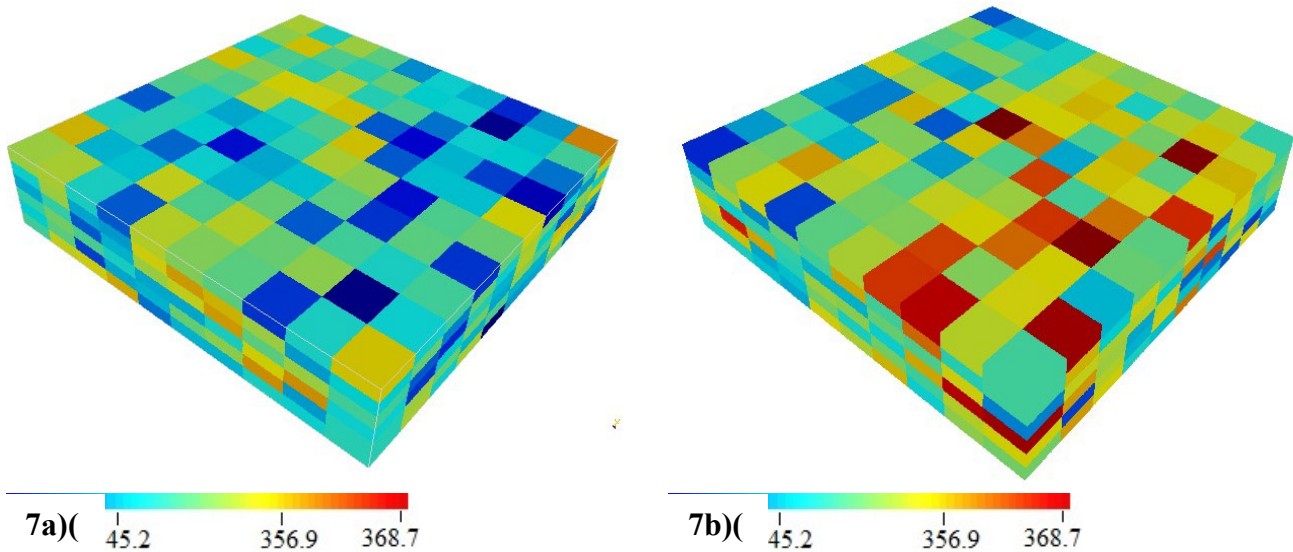


Figure 3. The most desirable static models. 7a) Permeability, 7b) Porosity

In order to better illustrate the difference between the models and the optimal model, the production index and the compressibility of the formation were used.

The production index, shown by J, is defined by Equations 17 and 18 [29,32].

$$J = \frac{Q_o}{P_r - P_{wf}} = \frac{Q_o}{\Delta P} \tag{Eq. 17}$$

$$J = \frac{0.00708k_o h}{\mu_o B_o \left[\ln \left(\frac{r_e}{r_w} \right) - 0.75 + s \right]} \tag{Eq. 18}$$

where $Q_o, P_r, P_{wf}, \Delta P, k_o, s, h$ respectively are oil flow rate, initial reservoir pressure, bottom-hole flowing pressure, drawdown, effective permeability of the oil, skin factor and thickness.

All reservoir parameters, including geometry, rock and fluid characteristics, type of fluid flow within the porous medium, are included in the production index. In fact, J represents all the properties of the reservoir.

According to equation 17 in constant rate production, the lower the drawdown, the higher and the production index will be. Based on this fact, the drawdown and production index for each model was calculated. Drawdown and Production index are given in Table 3 and the values were shown in Figures 8 and 9, respectively.

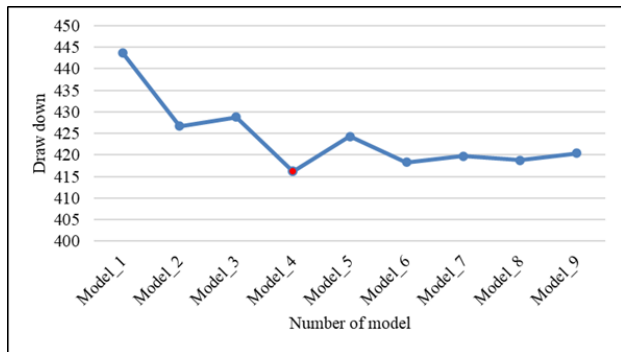


Figure 4. Draw down for 9 models

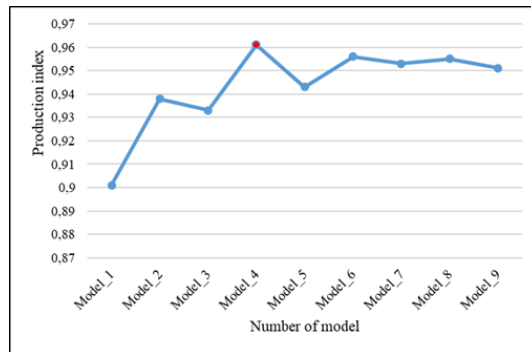


Figure 9. Production index for 9 models

When reducing SEE, bottom hole pressure (BHP) increased. Increasing BHP leads to reduce draw down and according to equation 17 leads to increasing production index from reservoir. Quantity of draw down in models 1 and 3 increased and these models have lowest amount of production index and highest BHP. Also the highest production index equals to 0.957 and belongs to model 4. This is the highest production index among other models.

According to equation 18, the production index is directly related to effective permeability of the oil. It can be concluded that the permeability rate of model number 4 is higher than other models. The effective permeability for all 5 models of permeability was shown in Figure 10. It is observed that permeability for model number 4 was had the highest value. The chart of model number 4 is shown with dashed line and the rest of the models are below it with smaller values. Which can be considered as one of the reasons for the inadequacy of permeability in other models. The formation compressibility can be used to compare porosity in models. The formation compressibility is indicated by C_f and defined by equation 19 [33].

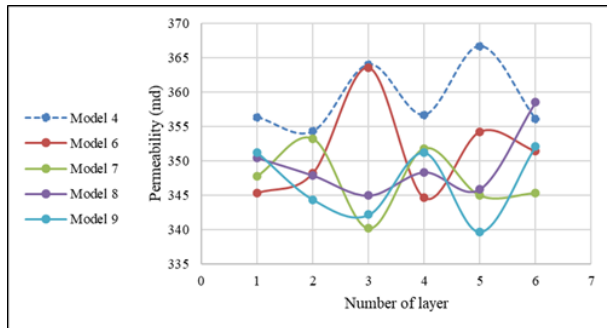


Figure 10. Effective permeability for 5 models in grid blocks of production well

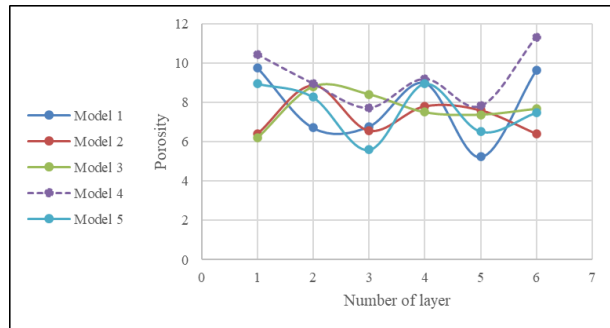


Figure 11. Porosity for 5 models in grid blocks of production well

$$c_f = \frac{1}{\phi} \cdot \frac{\partial \phi}{\partial P} \tag{Eq. 19}$$

The initial porosity is inversely related to pressure changes. In Figure 11 the porosity in grid blocks of production well for 5 static model is shown. The porosity of the model 4 with the dashed line is distinguished from other models and that is higher than other models.

3.3. Validation

Another simulation software, called eclipse, has been used to validate the simulated dynamic model. By using the same model of optimal porosity and permeability with respect to the remaining terms of discrete, single-phase and three-dimensional simulation of the eclipse was applied. Based on Figure 12, comparing the pressure from the production well column,

the difference between two methods is only 8 psi, which can be ignored. Figure 13 shows the reservoir pressure model in 3D for both methods, which was also confirmed the correctness of the built model.

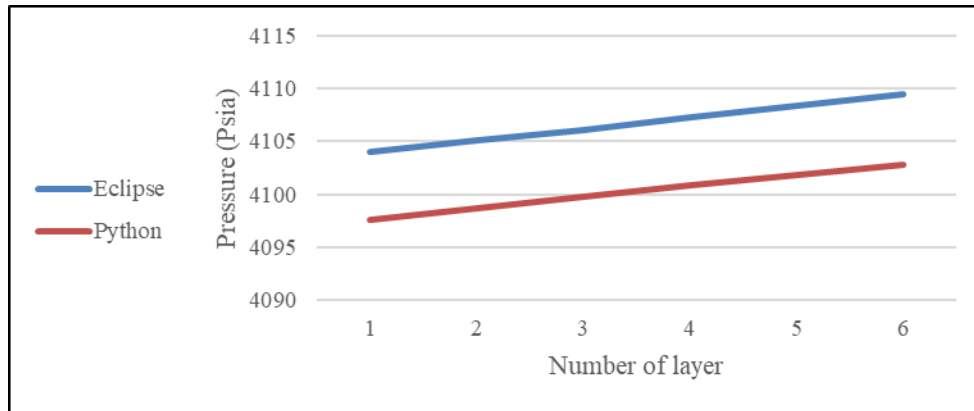
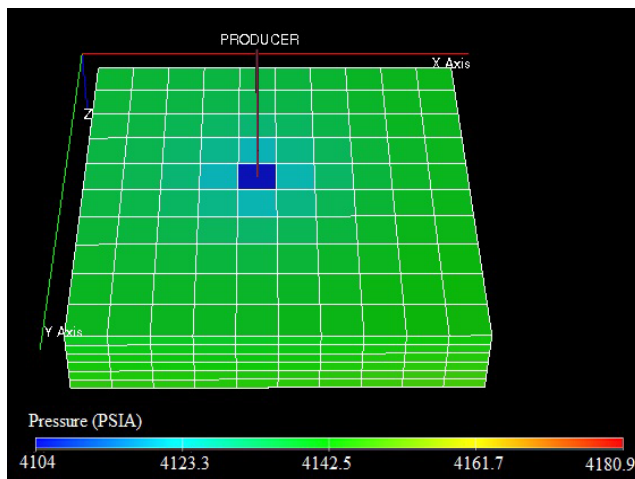
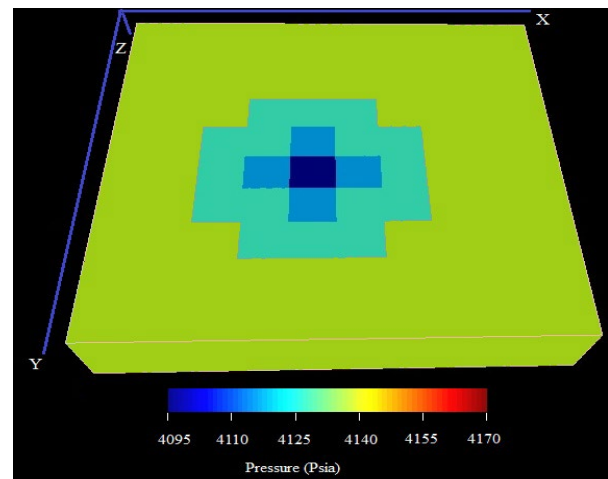


Figure 12. Comparison of pressure obtained for two methods



(13a)



(13b)

Figure 5. Comparison of pressure models obtained from Python code and Eclipse software. 13a) Pressure model obtained from Eclipse software. 13b) Pressure model obtained from Python code

4. Conclusion

In this study, an optimization algorithm was developed for finding the optimum static model using a combination of static and dynamic simulation techniques. After comparing different models by parameters such as SSE, bottom hole and drawdown pressures, production index and pressure of each block on production well, model No. 4, which is a simulation of the reservoir, has the lowest drawdown and SSE, and has been improved by 19.1% compared to the model with the highest SSE. It has also the highest production index and bottom hole pressure among the other dynamic models, which is the result of using the desired permeability and porosity.. The distinguishing feature of these dynamic models was their static models and the rest of the parameters were considered to be constant and the same. For this reason, the change in the results of the dynamic models was due to the change in their static models.

The desirability of the results of Model 4 depends on the desirability of its static model. This static model can be introduced as the most desirable static model for all two categories

of permeability and porosity data. With this method, a large number of static models in different dimensions can be compared according to the cost and time available. These models can be used for designing more reliable and suitable drilling sites for injection and production wells to produce more oil.

References

- [1] Abdollahzadeh A, Christie MAM, Corne D. Gaussian-based Estimation of Distribution Algorithms for History Matching, in: Abu Dhabi Int. Pet. Conf. Exhib., 2012: pp. 11–14. <https://doi.org/https://doi.org/10.2118/161951-MS>.
- [2] Hajizadeh Y, Christie MAM, Demyanov V, Engineering P. History matching with differential evolution approach; a look at new search strategies, in: SPE Eur. Annu. Conf. Exhib., 2010. <https://doi.org/https://doi.org/10.2118/130253-MS>.
- [3] Abdollahzadeh A, Christie M, Corne D, Davies B, Elliott MT. An Adaptive Evolutionary Algorithm for History-Matching, in: EAGE Annu. Conf. Exhib. Inc. SPE Eur., 2013. <https://doi.org/https://doi.org/10.2118/164824-MS>.
- [4] Cunha LB. Integrating static and dynamic data for oil and gas reservoir modelling, *J. Can. Pet. Technol.*, 2004; 43.
- [5] Thomas LK, Hellums LJ, Reheis GM. A Nonlinear Automatic History Matching Technique for Reservoir Simulation Models, *Soc. Pet. Eng. J.*, 1972; 12:508–514.
- [6] Watson AT, Lee WJ. A new algorithm for automatic history matching production data, in: SPE Unconv. Gas Technol. Symp., 1986. <https://doi.org/https://doi.org/10.2118/15228-MS>.
- [7] Ouenes A, Bhagavan S. Application of simulated annealing and other global optimization methods to reservoir description: myths and realities, in: SPE Annu. Tech. Conf. Exhib., 1994. <https://doi.org/https://doi.org/10.2118/28415-MS>.
- [8] Huang X, Kelkar MG. Application of combinatorial algorithms for description of reservoir properties, in: SPE/DOE Improv. Oil Recover. Symp., 1994. <https://doi.org/https://doi.org/10.2118/27803-MS>.
- [9] Velez-langs O. Genetic algorithms in oil industry: An overview, *J. Pet. Sci. Eng.*, 2005; 47 15–22. <https://doi.org/10.1016/j.petrol.2004.11.006>.
- [10] P.J. Ballester, J.N. Carter, A parallel real-coded genetic algorithm for history matching and its application to a real petroleum reservoir, *J. Pet. Sci. Eng.* 59 (2007) 157–168.
- [11] Mohamed L, Christie MA, Demyanov V. Comparison of stochastic sampling algorithms for uncertainty quantification, *SPE J.*, 2010; 15: 31–38.
- [12] L Mohamed L, Christie MA, Demyanov V. Engineering, Reservoir model history matching with particle swarms: Variants study, in: SPE Oil Gas India Conf. Exhib., 2010. <https://doi.org/https://doi.org/10.2118/129152-MS>.
- [13] Axmann JK, Haase O, Rian DT, Schulze-Riegert RW, Axmann JK, Haase O, You Y-L. Optimization methods for history matching of complex reservoirs, in: SPE Reserv. Simul. Symp., 2001. <https://doi.org/https://doi.org/10.2118/66393-MS>.
- [14] Hajizadeh Y, Christie MM., Demyanov V. Ant colony optimization algorithm for history matching, in: Eur. Conf. Exhib., 2009: pp. 1–13. <https://doi.org/https://doi.org/10.2118/121193-MS>.
- [15] Hamdi H, Hajizadeh Y, Sousa MC. Gaussian Process for Uncertainty Quantification of Reservoir Models, in: SPE/IATMI Asia Pacific Oil Gas Conf. Exhib., 2015: pp. 20–22. <https://doi.org/https://doi.org/10.2118/176074-MS>.
- [16] Sangyuhun L, Stephen KD, Sanghyun L, National K, Corporation O, Stephen KD. Optimising Automatic History Matching for Field Application Using Genetic Algorithm and Particle Swarm Optimisation, in: Offshore Technol. Conf. Asia, 2018. <https://doi.org/https://doi.org/10.4043/28401-MS>.
- [17] Tan TB. A computationally efficient Gauss-Newton method for automatic history matching, in: SPE Reserv. Simul. Symp., 1995: pp. 61–70. <https://doi.org/https://doi.org/10.2118/29100-MS>.
- [18] Schildberg Y, Poncet J, Bandiziol D, Deboaisne R, Laffont F, Vittori J. Integration of Geostatistics and Well Test to Validate a Priori Geological Models for the Dynamic Simulation: Case Study, in: SPE Annu. Tech. Conf. Exhib., 1997. <https://doi.org/https://doi.org/10.2118/38752-MS>.
- [19] Zhang F, Skjervheim JA, Risk S, As M, Reynolds AC, Oliver DS. Automatic history matching in a Bayesian framework, example applications, in: SPE Annu. Tech. Conf. Exhib., 2003. <https://doi.org/https://doi.org/10.2118/84461-MS>.

- [20] Zhang F, Reynolds AC. Optimization algorithms for automatic history matching of production data, in: Proc. 8th Eur. Conf. Math. Oil Recover., 2002: pp. 3–6.
<https://doi.org/https://doi.org/10.3997/2214-4609.201405958>.
- [21] Gao G, Reynolds AC. An improved implementation of the LBFGS algorithm for automatic history matching, in: SPE Annu. Tech. Conf. Exhib., 2004.
<https://doi.org/https://doi.org/10.2118/90058-MS>.
- [22] Aanonsen SI, Petroleum I, Nævdal G, Oliver DS, Reynolds AC, Vallès B. The ensemble Kalman filter in reservoir engineering--a review, Spe J., 2009; 14: 393–412.
- [23] Kalman RE. A new approach to linear filtering and prediction problems, J. Basic Eng., 1960; 82: 35–45.
- [24] Cohn SE. An Introduction to Estimation Theory (gtSpecial Issue>Data Assimilation in Meteorology and Oceanography: Theory and Practice), J. Meteorol. Soc. Japan. Ser. II.1997; 75: 257–288.
- [25] Leng CH, Yeh HD. Aquifer parameter identification using the extended Kalman filter, Water Resour. Res., 2003; 39(3).
- [26] Liang B, Alpak FO, Sepehrnoori K, Delshad M. A Singular Evolutive Interpolated Kalman Filter for Rapid Uncertainty Quantification, in: SPE Reserv. Simul. Symp., 2007: pp. 1–10.
<https://doi.org/https://doi.org/10.2118/106170-MS>.
- [27] Ertekin T, Abou-Kassem JH, King GR. Basic applied reservoir simulation, 2001.
- [28] Tanha AA, Zargar G, Mansouri M, Rahmati M. Comparison of Well Test Data with Reservoir Data Obtained by Well-Log, Using Well Test Software's and Presenting an Accurate Model According to Both Analytical Solution and Artificial Neural Network for Horizontal Wells in Naturally Fractured Reservoirs, Pet. Coal, 2022; 64(2): 387-405.
- [29] Aziz K, Settari A. Petroleum reservoir simulation, 1979.
- [30] MR Islam, SM Farouq Ali, Abou Kassem JH, Abou-kassem JH. Petroleum reservoir simulation: a Basic Approach, Gulf Publishing Company, 2006, ISBN-10: 0976511363.
- [31] Gerritsen MG, Durlofsky LJ. Modeling fluid flow in oil reservoirs, Annu. Rev. Fluid Mech., 2005; 37: 211–238.
- [32] Ayatizadeh Tanha A, Parizad A, Shahbazi K, Bagheri H. Investigation of trend between porosity and drilling parameters in one of the Iranian undeveloped major gas fields, Pet. Res., 2022; 64: 387–405.
- [33] Dandekar, AY. Petroleum reservoir rock and fluid properties, CRC press, 2013, eBook ISBN9780429109362.

To whom correspondence should be addressed: Dr. S. K. Abolfazli, Faculty of Mining, Petroleum and Geophysics Engineering, Shahrood University of Technology, Shahrood, Iran, Nigeria E-mail: s.abolfazli@yahoo.com